Journal of Drug Delivery Science and Technology 92 (2024) 105376

Contents lists available at ScienceDirect

Journal of Drug Delivery Science and Technology

journal homepage: www.elsevier.com/locate/jddst

Enhancing the safety and effectiveness of polyethylenimine gene delivery through cell membrane encapsulation

Mengying Wang, Yanlin Sun, Mingjie Wang, Zhaojun Yang, Yong Shi, Dong Zeng, Liang Liu *

School of Life Science and Technology, Wuhan Polytechnic University, Wuhan, 430023, China

ARTICLE INFO

Keywords:
Gene delivery
Polyethylenimine
Cell membrane
Cytotoxicity
Transfection efficiency

ABSTRACT

Due to the powerful DNA loading capacity and excellent proton sponge effect, the cationic polymer polyethyleneimine (PEI) has been demonstrated as a versatile, efficient DNA delivery tool both in vitro and in vivo. However, the excess surface positive charge of PEI and the common capture/clearance of PEI/DNA complex by the immune system limit its further clinical applications. To reduce the cytotoxicity resulting from surface charge and avoid the clearance of nanoparticles interacting with proteins and circulating immune cells in the blood, a bionic gene delivery system was developed by coating PEI/DNA complexes with natural cell membranes. The obtained RAW Cell membrane-coated PEI/DNA capsules (RAWm-PDc) and Red blood Cell membrane-coated PEI/DNA capsules (RBCm-PDc) complex showed excellent dispersibility and stability with an average particle size of 200–300 nm. Moreover, the RAWm-PDc/RBCm-PDc complex had great DNA loading capacity and protected the bound DNA effectively from nuclease hydrolysis. Most importantly, the RAWm-PDc/RBCm-PDc complex exhibited low protein adsorption, reduced cytotoxicity and high gene delivery efficiency. All the results demonstrated the potential of RAWm-PDc/RBCm-PDc as a promising non-viral gene delivery vector.

1. Introduction

Gene therapy represents a new disease treatment strategy by delivering genetic material into specific cells to restore abnormal activity [1,2]. It is widely recognized that genetic abnormality results in a variety of diseases, including cancers [3]. Over the past decades, gene therapy has been greatly developed and was considered as a safe and effective treatment option for cancer [4]. So far, it has been reported gene therapy is used to treat malignant tumors via the way of gene immunization, gene knockout, gene modification, or gene supplementation [5–7]. Among the factors which greatly affect gene therapy, proper gene delivery tool is one of the most critical factors [8]. Therefore, developing a safe and efficient delivery vector for gene therapy is a challenge that remained to be addressed [9].

There are two main tools which are broadly exploited for gene delivery, viral and non-viral types [10]. In general, viral vectors can effectively encapsulate and deliver genetic material into cells, however, the high immunogenicity, risk of insertional mutagenesis and weak targeting ability prevent them from being ideal gene delivery vectors for clinical applications [11–13]. Compared to viral vectors, non-viral vectors have certain advantages, for instance, low immunogenicity, reduced cytotoxicity, higher safety, and application on a large scale [14–16]. The development of non-viral vectors to be safe and efficient gene carriers has attracted great interest in the gene therapy field [16,17]. Among various non-viral gene vectors, the polycationic polymer Polyethyleneimine (PEI) has appealed to researchers over the past years due to its strong DNA compaction capacity and versatile chemical modification options [18–20]. PEI forms complex with the negatively charged genetic material and deliveries to the targeted cells [21]. However, a few drawbacks still accompany non-modified PEI such as cytotoxicity (depending on excessive surface cationic charge), and aggregation under high ionic strength conditions [22]. In addition, opsonization and short-term stability further limit its use for nucleic acid delivery. Therefore, additional modifications are required to qualify PEI for being used as a gene carrier [23,24].Recently, common grafting or embedding strategies for PEI modifications have been applied to enhance its biocompatibility, decrease its cytotoxicity and improve its transfection efficiency [25–28].

Based on the emergence of new engineering technologies and a deeper understanding of natural cellular functions, bionic delivery systems have rapidly become a new research sensation by mimicking biological particles such as cells and viruses [29–32]. In particular, cell

* Corresponding author.
E-mail address: hustll@126.com (L. Liu).

https://doi.org/10.1016/j.jddst.2024.105376
Received 29 September 2023; Received in revised form 7 January 2024; Accepted 12 January 2024
Available online 12 January 2024

membrane-encapsulated nanoparticles are a gratifyingly efficient biomimetic strategy [33]. Polymer/DNA complexes coated with cell membranes gain the ability to evade clearance by the immune system and specific delivery to target cells with enhanced stability [34]. The application of cell membranes as a safe material in gene delivery has been explored by utilizing different cancer cell membrane-encapsulated PEI/DNA complexes to prepare safe and efficient gene delivery systems and to probe their safety and homologous targeting in past work [35]. Cell membrane from different cell types has been investigated for nanoparticle coating, including red cell membrane, white cell membrane, cancer cell membrane and so on [36,37]. Notably, the unique physicochemical properties and biological functions possessed by erythrocytes provide more possibilities for the development of gene delivery, and thus biomimetic strategies based on erythrocyte membrane-coated nanoparticles have received further attention. The erythrocyte membrane enables the nanoparticles to be separated from their surroundings, thus achieving an "invisibility effect" in vivo and avoiding recognition by macrophages [33]. Hu et al. first proposed to develop a red blood cell membrane-camouflaged polymer nanoparticle platform for long-term cyclic cargo delivery by coating natural red blood cell membranes on biodegradable polymer nanoparticles via a top-down approach [38]. Gao et al. reported a biomimetic drug delivery system based on macrophage membrane preparation [39]. The macrophage membrane was able to effectively avoid the removal of nanoparticles by the reticuloendothelial system and also directed nanoparticles to the inflamed tissues [40]. Interestingly, macrophages membrane coating greatly prolonged the circulation time of coated polymers, more than 30 % coated polymer remained free after 24h post in vivo treatment, meanwhile, almost all uncoated polymer were engulfed [41,42].

In present work, an effective and facile cell membrane-coated biomimetic strategy is utilized to optimize nanoparticles as a promising tool for gene delivery. Importantly, mature erythrocytes do have no genetic material and are therefore completely biodegradable and do not produce any toxic substances, which makes red blood cell membranes (RBCm) safer for use in delivery systems. Meanwhile, RBCm can be easily separated in hypotonic solution and purified by hemolysis to encapsulate PEI/DNA complexes (RBCm-PDc). As a control, mouse mononuclear macrophage membranes (RAWm) were extracted to encapsulate PEI/DNA complexes (RAWm-PDc). The obtained RBCm-PDc/RAWm-PDc complexes from the encapsulation of PEI10k/DNA and PEI25k/DNA complexes with purified RBCm and RAWm under the optimal mass ratio were characterized by SDS-PAGE electrophoresis, particle size potential analysis, and atomic force microscopy. At the same time, complexes stability was analyzed by DLS assay in which the particle size of the complexes over a period of 28 days and the potential change were measured. DNA loading capacity, protective effect and release ability of those complexes were addressed by agarose gel assays. The core properties, cytotoxicity, and in vitro cellular uptake/transfection efficiency, were measured by MTT assay, fluorescent microscopy and flow cytometry, respectively. In sum, cell membrane coating greatly reduced cytotoxicity, and significantly enhanced cellular uptake and transfection efficiency, therefore, the novel cell membrane-coated PEI can be further analyzed as a safe and efficient gene delivery tool in vivo.

2. Materials and methods

2.1. Reagents

Branched polyethyleneimine (bPEI, Mw = 10, 25 kDa) was purchased from Macklin Biochemical Co., Ltd. (Shanghai, China). Fluorescein isothiocyanate (FITC), ethidium bromide (EtBr) fluorescent dyes, and DiI (CM Red Fluorescent Probe) were obtained from Sigma-Aldrich (Shanghai, China). The EGFP plasmid was amplified in Escherichia coli and purified using a Maxi plasmid kit from Tiangen Biotech Co., Ltd. (Beijing, China). 3-mercaptopropionic acid (MA), glutathione (GSH), and dimethyl sulfoxide (DMSO) were purchased from Shanghai Macklin Biochemical Technology Co., Ltd. 3-[4,5-dimethylthiazol-2-yl]-2,5-diphenyltetrazolium bromide (MTT) and fetal bovine serum (FBS) were obtained from China National Pharmaceutical Group Corporation (Shanghai, China). Dulbecco's modified Eagle's media (DMEM) and Active Ingredient-Active Ingredient solution (100 ×) were purchased from Gibco (Shanghai, China).

2.2. Cell culture

HEK-293T and HeLa cells were obtained from the National Center for Cell Repository (Beijing, China) and cultured in DMEM containing 10% FBS and 1 % Active Ingredient-Active Ingredient at 37 °C in a 5 % CO_2 humidified incubator.

2.3. Preparation

2.3.1. RAW/RBC cell membrane isolation

RAW cells were cultured and harvested at the density of 80–90 %. After centrifugation, cells were resuspended in pre-cold isotonic PBS (pH = 7.4) at 4 °C, then centrifuged at 1000 rpm for 3 min at 4 °C, and repeated the washing step 2–3 times. Afterwards, cells were resuspended in pre-cold 0.25 × PBS and incubated for 1 h at 4 °C. Then, cell suspension was frozen in ultra-low temperature refrigerator for 10 min and placed at room temperature to thaw, repeated this freezing and thawing step five times. After centrifugation at 15000 rpm for 10 min at 4 °C, cell membrane precipitates were collected, then freeze-dried and prepared as 1 mg/mL RAWm solution in sterile water. The obtained RAWm solution was stored at −20 °C for further use.

Red blood cell membranes were prepared by the hypotonic method. Whole blood was taken from the orbital plexus of rats, and the upper plasma layer was removed after centrifugation at 3000 rpm for 5 min at 4 °C, and the resulted erythrocyte precipitate was washed 2–3 times with isotonic PBS (pH = 7.4) solution until the supernatant colorless. Then, cells were resuspended with pre-chilled 0.25 × PBS solution at 4 °C and subjected to hypotonic lysis at 4 °C. The released hemoglobin was removed by centrifugation at 15000 rpm for 5 min, after sufficient rupture of erythrocytes in a hypotonic environment. The light pink erythrocyte membrane was collected after centrifugation and washed 2–3 times with 1 × PBS solution. The cell membrane precipitate was resuspended in deionized water and freeze-dried to obtain solid RBCm fragments.

2.3.2. Preparation of Dil-RAWm/RBCm and FITC-PEI

10 ml 1 mg/mL RAWm solution and 10 μl 5 mmol/L Dil solution were added to the beaker and stirred at room temperature for 4h under dark. The resulting mixture was centrifuged at 15000 rpm for 10min at 4°Cand then washed 2–3 times with deionized water until the supernatant colorless. 10 ml deionized water was added to resuspend the precipitate to obtain 1 mg/ml Dil-labeled RAWm. The Dil-labeled red blood cell membranes were prepared in the same way.

10 mg PEI25k was dispersed in 10 ml deionized water, and 2 ml 5 mg/ml FITC solution was added. The mixture was stirred under dark at RT for 24 h, then the mixture was placed in a 1000Da dialysis bag and water-dialyzed for 48 h to remove free FITC. The retentate was collected and diluted with deionized water to final concentration 1 mg/ml to obtain the FITC-labeled PEI.

2.3.3. Preparation of RAWm-PDc/RBCm-PDc complexes

The amount of DNA in each group was 0.4 μg, and the mass ratio of PEI10k/DNA was 1/1, 1.5/1, 2/1, 2.5/1, 3/1, 3.5/1, that of PEI25k/DNA was 0.5/1, 1/1, 1.5/1, 2/1,3/1. After 60min incubation at room temperature for complete binding between PEI and DNA, 2 μl 6 × loading buffer was added and mixed. Then the samples were added into 1 % agarose gel for the electrophoresis at 120 V. The gel was observed with Bio-Rad imaging system. After determination of optimal PEI/DNA binding ratio, PEI/DNA complex was coated with cell membranes.

As shown in Scheme 1, RBCm-P10Dc and RBCm-P25Dc complexes were prepared by the extrusion method. RBCm was sonicated for 5min at room temperature and then mixed with PEI/DNA complex at different mass ratios, where the mass ratios of RBCm/PEI10k/DNA were 0.5/2/1, 1/2/1, 2/2/1, 3/2/1, 4/2/1, and the mass ratios of RBCm/PEI25k/DNA were 0.5/1/1, 1/1/1, 2/1/1, 3/1/1, and 4/1/1. After 30min incubation at room temperature, RBCm/PEI/DNA complex was extruded through a polycarbonate membrane with 200 nm pore size using a Genizer liposome extruder to produce the RBCm-PDc complex, which was repeatedly extruded 10 times and then stored at −20 °C. The RAWm-PDc complexes were prepared in the same way.

2.4. Characterization

2.4.1. SDS-PAGE

Polyacrylamide gel electrophoresis (SDS-PAGE) was used to determine the protein retention on the surface of the RAWm-PDc/RBCm-PDc complex. The retention of membrane proteins was determined by SDS-PAGE electrophoresis to analyze proteins of RAW cells, RAWm, RBC cells, RBCm, RAWm-PDc complexes, and RBCm-PDc complexes. 40 μl 1 mg/ml RAWm-PDc complex and RBCm-PDc complex were mixed with 10 μl 5 × upper sample buffer and then boiled in the water bath for 10 min. After the short centrifugation, 20 μl supernatant was added. The samples were electrophoresed at 80V for 30min until reaching the concentrate gel, and further electrophoresed at 120 V for 2h. The gels were then stained for 2h in Komas Brilliant Blue and decolorized with decolorizing solution, and imaged with the gel imaging system (Gel Doc XR, Bio-RadUS).

2.4.2. Particle size and zeta potential

The particle size and zeta potential of RAWm, RAWm-PDc complexes and PEI/DNA complexes were determined by dynamic light scattering (DLS). The amount of DNA in each sample was 1 μg and the total volume was 4 ml, where the mass ratio of RAWm/PEI10k/DNA was 0.5/2/1, 1/2/1, 2/2/1, 3/2/1, 4/2/1 and the mass ratio of RAWm/PEI25k/DNA was 0.5/1/1, 1/1/1, 2/1/1, 3/1/1, 4/1/1. The mean particle size and surface zeta potential of complexes at 25 °C were measured by the dynamic light scattering particle sizer.

2.4.3. AFM

The morphology of RAWm-PDc, RBCm-PDc complexes was observed by AFM. The prepared complexes were diluted with deionized water to the appropriate concentration, afterwards 50 μl complex solution was added dropwise to the treated mica sheets, dried at room temperature and measured by atomic force microscopy using a silicon cantilever. The AFM height profile was analyzed and quantified using Gwyddion (Version 2.58) software.

2.5. Stability analysis

DLS (Zetasizer Nano ZS (Malvern, U.K.))was used to monitor the change of particle size and zeta potential of RAWm-PDc and RBCm-PDc complexes over a period of one month to evaluate the complexes' stability. RAWm-P10Dc complexes with mass ratio 3/2/1 (RAWm-P25Dc complexes with mass ratio 2/1/1) were prepared according to the method in section 2.4 and then dispersed in isotonic PBS buffer and placed at 4 °C. In the end, the particle size and zeta potential of complexes were examined at the 0, 7, 14, 21, and 28 day using dynamic light scattering particle sizer (Zetasizer Nano ZS (Malvern, U.K.)). The same method was used to determine the particle size and potential changes of the RBCm-PDc complex over a period of 28 days.

2.6. BSA adsorption

The protein adsorption capacity was determined by spectroscopic method, and the standard curve was plotted according to the absorbance of BSA standard solution after reaction with G250 solution. PEI was used as the control group. 1 ml 1 mg/ml RAWm-PDc (RBCm-PDc) solution was incubated with 1 ml 1 mg/ml BSA solution for 30 min at 37 °C, followed by centrifugation at 10000 rpm for 10 min. Then 30 μl supernatant was added to 1 ml G250 solution, mixed and incubated for 5 min. The absorbance was measured at the wavelength of 595 nm, and the BSA concentration was calculated by the standard curve. The protein adsorption rate was calculated according to formula (2), in which m_0 is the mass of BSA added to the carrier and m is the mass of BSA in the supernatant.

$$\text{Adsorption rate } (\%) = \frac{m_0 - m}{m_0} \times 100\ \% \quad (1)$$

2.7. Encapsulation rate (EE) determination of RAWm-PDc/RBCm-PDc complex

The optimal binding ratio of cell membrane with PEI/DNA complexes and the optimal extrusion repeats were investigated by encapsulation rate determination. PEI10k/DNA complexes with mass ratio 2/1 (PEI25k/DNA complexes with mass ratio 1/1) were prepared with DAPI-labeled DNA, and the fluorescence intensity of PEI/DNA complexes at 454 nm (λex = 364 nm) was measured by a multifunctional microplate reader (EnSpire™, PerkinElmer US). RAWm-P10Dc (mass ratios 0.5/2/1, 1/2/1, 2/2/1, 3/2/1, 4/2/1), RAWm-PEI25Dc (mass ratios 0.5/1/1, 1/1/1, 2/1/1, 3/1/1, 4/1/1) were prepared according to the method in section 2.4. Then, the RAWm-PDc complexes with different mass ratios and different numbers of extrusions were produced by repeated extrusion 5,10,or 15 times. The fluorescence intensity of the supernatant at 454 nm was measured after 10 min centrifugation at 15000 rpm, and the encapsulation rate of RAWm on PEI/DNA complexes was calculated according to Equation (1). The same method was used to determine the encapsulation rate of RBCm on PEI/DNA complexes.

EE (%) = ((PEI/DNA fluorescence intensity - supernatant fluorescence intensity)/PEI/DNA fluorescence intensity) × 100% (2)

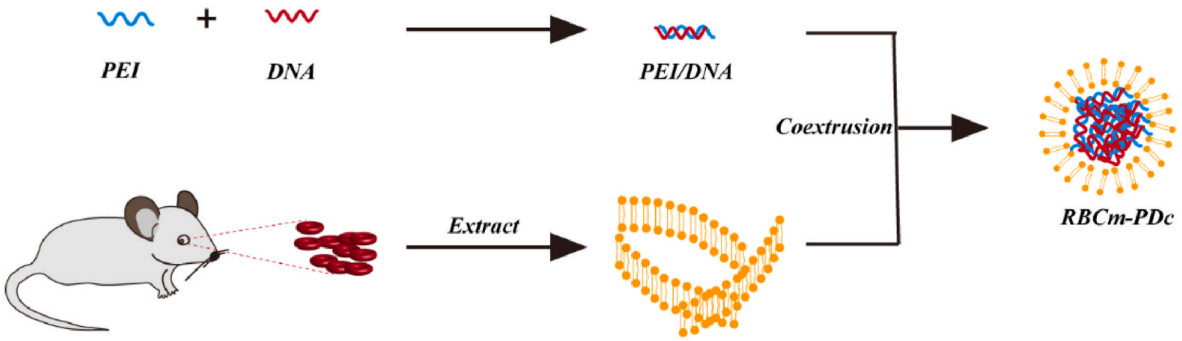

Scheme 1. Preparation of RBCm-PDc.

2.8. Protection and release of DNA

The protection and release ability of DNA within RAWm-PDc/RBCm-PDc complexes was evaluated by agarose gel electrophoresis. RAWm-P25Dc and RBCm-P25Dc complexes made in section 2.4 were compared with PEI25k/DNA alone, while bare DNA as blank control and 0.4 μg DNA per sample was used. Five groups were prepared, GroupI was control without any treatment. In group II, 2.5 μl 40 U/ml nuclease (DNaseI) and 2.5 μl 10 × Reaction Buffer were added, mixed and incubated at 37 °C for 2h. In group III, 8 μl 20 mg/ml Active Ingredient sodium solution was added, mixed and incubated at 37 °C for 2h. In group IV, 2.5 μl 40 U/ml DNaseIand 2.5 μl 10 × Reaction Buffer was mixed and incubated at 37 °C for 2h, then 2 μl 5 mM/L EDTA was added and incubated at 65 °C for 10 min to inactivate DNaseI, and 8 μl 20 mg/ml sodium Active Ingredient solution was added and incubated at 37 °C for 2h. In group V, 8 μl 20 mg/ml sodium Active Ingredient solution was incubated for 2 h at 37 °C, followed by the addition of 2.5 μl 40 U/ml DNaseI and 2.5 μl 10 × Reaction Buffer for 2 h at 37 °C. 2 μl 6 × Loading buffer was added to each group and then added to the gel. After 40 min electrophoresis at 120 V, the results were observed with a gel imaging system (Bio-Rad).

2.9. Cytotoxicity

The MTT assay was used to investigate the toxicity magnitude of RAWm, RBCm, PEI and RAWm-PDc/RBCm-PDc complexes with different mass ratios in HEK-293T cells and Hela cells. The amount of control ctDNA was 1 μg per well. Cells were seeded in 96-well plates at the density of 1×10^4 cells per well and cultured for 24 h. Afterwards, each complex was added to cells and incubated for another 48h, the culture medium without any complex was used as control. Then, 100 μl DMEM medium containing 0.5 mg/ml MTT was added and incubated for 4h. After this, 100 μl DMSO was used and shaken for 10 min until the blue-purple methylzan crystals were completely dissolved. The absor-bance of each sample at 570 nm was measured via a multifunctional microplate reader (EnSpire™, PerkinElmer, USA). For each group, triplicate were set for the measurement and analysis, the data were calculated the mean viability with standard deviation. Cell viability was analyzed according to formula (3), where A_0 was the absorbance at 570 nm which treated with complete medium, and A was the absorbance at 570 nm which treated with the various complex.

$$\text{Cell viability}(\%) = \frac{A}{A_0} \times 100\% \quad (3)$$

2.10. Cellular uptake of RAWm-PDc, RBCm-PDc complexes

HEK-293T cells and Hela cells were used to measure the uptake efficiency of the complex in normal and cancer cells. 10 mg FITC dissolved in 2 ml DMSO was mixed with 10 ml 1 mg/ml PEI10k (PEI25K) solution, stirred under dark at room temperature for 24h, then placed in a 1000Da dialysis bag and dialyzed in running water for 48h. The retention solution was collected and freeze-dried to obtain FITC-labeled PEI (FITC-PEI). Dil and FITC labeled RAWm-PDc (RBCm-PDc) complexes with different mass ratios were prepared according to the procedure in section 2.4, and FITC-PEI/DNA complexes were used as control. For each group, 2 μg ctDNA per well was used.

When cells in each well reached 80%–90 % confluence, 1 ml DMEM medium containing complex was added and incubated for 4–6 h. Then, DMEM medium containing complex was removed and cells were fixed in 300 μl paraformaldehyde solution for 15 min. Afterwards, cells were washed 3 times with PBS, and 300 μl 15 μg/ml DAPI solution was added. 10min later, DAPI solution was removed and cells were washed 3 times using HBSS buffer. The coverslips were placed on glass slides containing glycerol and the uptake of the different complexes by HEK-293T cells was observed under laser confocal microscopy (CLSM). To quantify the uptake efficiency of complexes, cells were cultured in DMEM medium containing the complex for 4–6h, then cell suspensions were prepared and the cellular uptake of complex was measured by flow cytometry (CytoFLEX, BECKMAN, US).

2.11. In-vitro transfection ability of RAWm-PDc and RBCm-PDc complexes

To investigate the transfection efficiency of RAWm-PDc and RBCm-PDc complexes in vitro, enhanced green fluorescent protein (EGFP) plasmid was employed as the reporter genes. RAWm-PDc (RBCm-PDc) complexes with different mass ratios were prepared according to the procedure in section 2.4, and PEI/DNA complexes were used as control. For each group, 1 μg DNA per well was used. Cells were grown to the density of 80 %, DMEM medium containing the complex was added and incubated for 4–6 h. Then, DMEM medium with complex was carefully replaced by 1 ml DMEM medium with 10 % serum but without Active Ingredient-Active Ingredient. After 48h incubation, the expression of EGFP was observed by fluorescence microscopy. Flow cytometry was used to quantify the efficiency of EGFP gene expression in cells. The average fluorescence intensity was analyzed by image J software.

2.12. Statistics and software

Statistical analysis was performed using GraphPad Prism software. Data were analyzed using Student *t*-test and one-way analysis of variance (ANOVA). $p < 0.05$ was considered statistically significant.

3. Result and discussion

3.1. Preparation

To address the potential of RAWm-PDc and RBCm-PDc as safe and efficient gene vectors, DNA loading ability of different-molecular-weight PEI with different mass ratios was investigated by agarose gel electrophoresis and the optimal mass ratios of PEI/DNA were selected for subsequent studies. From Fig. 1(a and b), it clearly shown that with different mass ratios, DNA bound with PEI10k and PEI25k gradually increased and then decreased. The maximal DNA binding with PEI10k was that at the mass ratio 2/1, and with PEI25k was that at the mass ratio 1/1. Therefore, mass ratio 2/1 (PEI10k/DNA) and 1/1 (PEI25k/DNA) was used as the optimized mass ratio in the following experiments.

3.2. SDS-PAGE

After complexes preparation, to verify the isolated cell membrane and whether the membrane coating in RBCm-PDc complexes was fully achieved, the protein composition of the complexes was analyzed by SDS-PAGE. As shown in Fig. 1c, RBCm and RAWm had similar protein composition as the original RBC cells and RAW cells, respectively, even though a few protein bands of RBCm and RAWm were missing or the protein amount was different, this could be due to the partial membrane protein loss during the extraction process. As the RAWm-PDc complex and the RBCm-PDc complex underwent multiple extrusion repeats by the liposome extruder, it resulted in the slightly more membrane proteins loss. However, most of the membrane proteins were still retained, indicating that the major properties of the cell membrane in the RAWm-PDc and RBCm-PDc complexes were not greatly altered.

3.3. Particle size and zeta potential

Among the factors affecting the cellular uptake of vector/DNA complex, the particle size is a important one. As observed in Fig. 1(d and e), the average particle size of all RAWm-PDc and RBCm-PDc complexes with different mass ratios were varied between 200 nm and 300 nm,

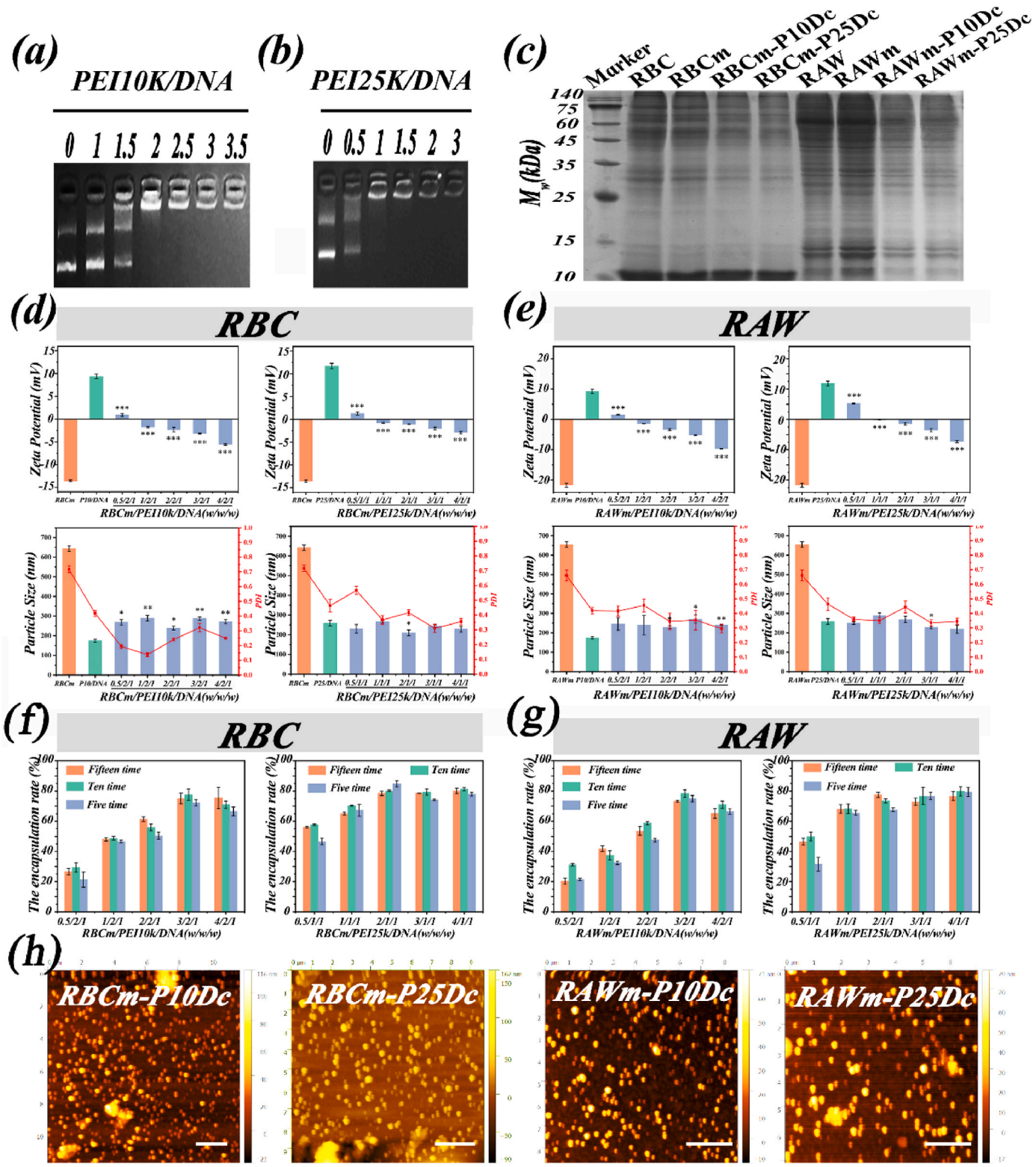

Fig. 1. Characterization of RAWm-PDc and RBCm-PDc. (a) Agarose gel electrophoresis result of PEI10K/DNA complexes with different mass ratio; (b) Agarose gel electrophoresis result of PEI25K/DNA complexes with different mass ratio; (c) SDS-PGE electrophoresis result of RBCm, RBCm-PDc, RAWm and RAWm-PDc; (d) Particle size and Zeta potential of RBCm complexes; (e) Particle size and Zeta potential of RAWm complexes; (f) the encapsulation rate of RBCm complexes; (g) the encapsulation rate of RAWm complexes; (h) AFM measurement of RAWm-PDc and RBCm-PDc.

which was favorable for cellular uptake. More importantly, the polydispersity coefficients PDI of all the complexes were distributed in the range of 0.1–0.4, which indicated that the complexes were well dispersed and not prone to aggregation.

In addition, since the zeta potential of polymers was related to cytotoxicity, and the high surface charge of polymers frequently leads to cytotoxicity, the zeta potential of obtained polymers was measured. As shown in Fig. 1(d and e), the PEI/DNA complex exhibited high zeta

potential, while the zeta potential of RAWm-PDc and RBCm-PDc complexes was gradually decreased when RBCm and RAWm amounts used for coating were increased, this result indicated that cell membrane coating significantly reduced the zeta potential of complexes, therefore it can be hypothesized that the cytotoxicity of the complex is also reduced.

3.4. AFM

The morphological results of RAWm-PDc and RBCm-PDc complexes were shown in Fig. 1h. RAWm-PDc and RBCm-PDc complexes were generally spherical or ellipsoidal, with diameters between 50 and 200 nm, which were consistent with the DLS particle size data. In addition,

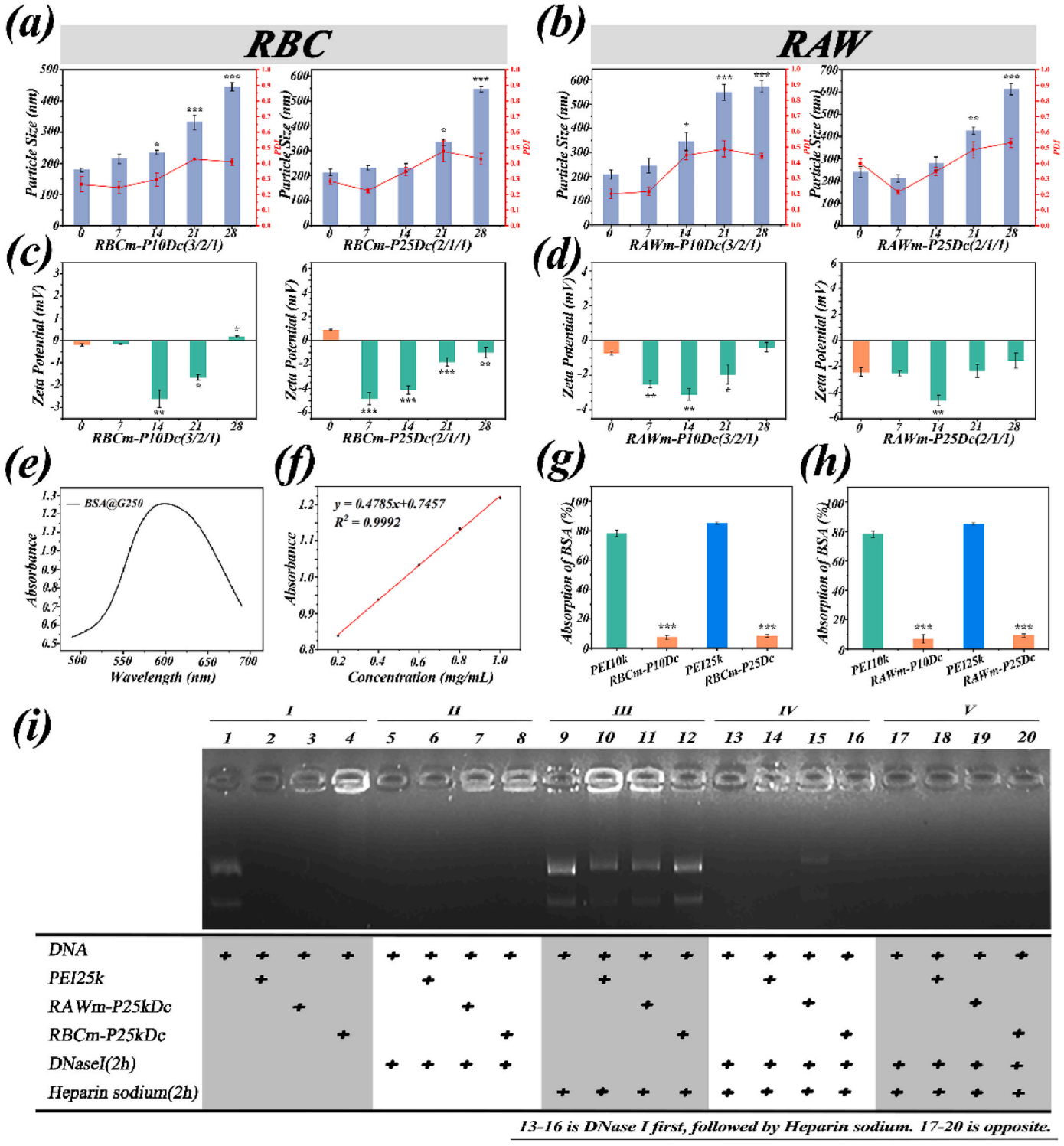

Fig. 2. The stability, protein absorption and protective effect of RAWm-PDc and RBCm-PDc. Particle size (a–b) and zeta potential (c–d) of RAWm-PDc and RBCm-PDc complexes at one month after binding at optimal mass ratio. (e) UV–Vis absorption spectrum of BSA@G250. (f) Standard curve of BSA and G250 mixed system. (g–h) Adsorption capacity of RAWm-PDc and RBCm-PDc on BSA. (i) Agarose gel electrophoresis results in DNA protection and release ability of RAWm-PDc and RBCm-PDc complexes.

The particle size of each complex suggested there was no obvious complex aggregation formed.

3.5. DNA encapsulation efficiency

As the gene carrying ability of nano-particles is dependent on their DNA encapsulation efficiency, in this study, the mass ratios between cell membrane and PEI/DNA complex, and the number of extrusion repeats which greatly mediate DNA encapsulation were investigated. As shown in Fig. 1(f and g), the encapsulation rates of RBCm-PDc and RAWm-PDc complexes were determined by mass ratio and the number of extrusion repeats. The encapsulation efficiency of RBCm-P10Dc and RBCm-P25Dc reached the maximal values at mass ratio 3/2/1 and 2/1/1, 75.62 % and 80.31 %, respectively. Coming to RAWm-P10Dc and RAWm-P25Dc, the greatest encapsulation efficiency was 72.74 % and 77.63 % at mass ratio 3/2/1 and 4/1/1, respectively. Interestingly, in most of the cases, 10 extrusions exhibited greater DNA encapsulation rate than either 5 extrusions or 15 extrusions, therefore, 10 extrusions is used as the optimized condition for complex preparation.

3.6. Stability

The stability of the polymer under physiological conditions is critical for the development of promising gene delivery tools, the stability of RAWm-PDc and RBCm-PDc complexes was measured by analyzing the particel size change within a certain period of time. As shown in Fig. 2(a and b), the particle size of RBCm-P10Dc and RBCm-P25Dc complexes was kept around 200 nm at the first 14 days, then increased to 450 nm for RBCm-P10Dc and 550 nm for RBCm-P25D at day 28. Meanwhile, the particle size of the RAWm-P25Dc complex remained around 200 nm for the first 14 days whereas the particle size of the RAWm-P10Dc complex increased to 344 nm by day 14. The zeta potential of complexes were changed during the incubation. As seen in Fig. 2(c and d), for the tested polymers, the zeta potential was decreased and reached the minimal value at day 14, then converted to increase during further incubation. Combined with the data in Fig. 2a–d, the RAWm-PDc/RBCm-PDc complex maintains a highly desirable steady state during the first 7 days.

3.7. BSA adsorption

Nanoparticles are prone to interact with proteins in the blood during systemic circulation and lead to thrombosis or allergic reactions, so exploring the adsorption ability of the complexes with proteins is beneficial for the design and synthesis of gene delivery vectors. As shown in Fig. 2(e and f), the maximum absorption wavelength was 595 nm after the reaction of BSA with G250, and a good linear relationship between the concentration of BSA standards and the absorbance at 595 nm was observed. Importantly, as can be seen from Fig. 2(g and h), PEI10k and PEI25k had high adsorption rates for BSA, 78.25 % for PEI10k and 85.19 % for PEI25k, but, the adsorption rate of RAWm-PDc/RBCm-PDc complex was significantly reduced to about 10 %. In conclusion, compared to PEIs, RAWm-PDc/RBCm-PDc complex had lower adsorption capacity, which made it suitable for the following in vitro cell experiments.

3.8. DNA protection and release

An ideal gene delivery vector not only protect the bound DNA from hydrolyzed by the nucleases during the circulation in the body, but also can efficiently release the carried DNA after entering into the cells. Here, the protective effect and release ability of PEI25k, RAWm-PDc/RBCm-PDc complexes were evaluated by agarose gel electrophoresis.

As seen in Fig. 2i, in group I, DNA in lane 1 which was bare DNA shown clear bands, and DNA in lanes 3 and 4 were completely retained in the wells. In group II, the result represented the samples treated by nuclease. As expected, the bare DNA was completely hydrolyzed by nuclease, therefore no bands remained in lane 5, however, there was fluorescence detected in lanes 6–8, suggesting that DNA bound in the complexes was not recognized and hydrolyzed by nuclease DNase, which confirmed the protective effect of PEI25k/DNA, RBCm-P25Dc and RAWm-P25Dc complexes. In group III, there were clear bands observed in lanes 9–12, in which samples were treated by sodium Active Ingredient This result indicated that applied to sodium Active Ingredient can efficiently displace DNA from the complexes. In group IV, all the samples were firstly treated with nuclease, then incubated with sodium Active Ingredient. The bands in lanes 14–16 further confirmed the protective effect of the complexes, and efficient release of DNA from the complexes by sodium Active Ingredient. In contrast, in group V, all the samples were treated by sodium Active Ingredient, then incubated with nuclease, the released DNA resulted from sodium Active Ingredient treatment was degraded by nuclease, therefore no bands were observed in lanes 17–19. In sum, PEI/DNA, RAWm-P25kDc and RBCm-P25kDc complexes exhibited protective ability of the bound DNA.

3.9. Cytotoxicity

Additionally, the cytotoxicity of RAWm, RBCm, RAWm-P10Dc, RAWm-P25Dc, RBCm- P10Dc, as well as RBCm-P25Dc was evaluated in both HEK-293T and HeLa cells by MTT assay. As reported in Fig. 3a, there is no severe cytotoxicity of RAWm and RBCm was observed in Hela cells, even under high concentration. In particular, the survival rates of cells that were treated with 25 μg/mL RBCm was 97 %, and low con-centration RBCm slightly promoted cell proliferation. Meanwhile, the cytotoxicity of PEI10k and PEI25k was correlated with the concentra-tion, cell survival rates under treatment of 25 μg/mL PEI10k and PEI25k were 60 % and 52 %, respectively. This result demonstrated that PEI is not an ideal gene delivery vector because of its high cytotoxicity and further modifications were required. With the mass weight increase of RBCm and RAWm, cell survival rates were gradually elevated and then reached the maximal values. As shown in Fig. 3c, the maximal cell survival rates of RAWm-P10Dc and RBCm-P10Dc were 84.2 % and 83.7 %, with 21.7 % and 21.1 % increase compared to the controls, respec-tively. In parallel (Fig. 3e), the maximal cell survival rates of RAWm- P25Dc and RBCm-P25Dc were 81.9 % and 82.1 %, with 28.1 % and 28.3 % increase compared to the controls, respectively. All the data suggested that cell membrane encapsulation can efficiently reduce cytotoxicity. Interestingly, cell membrane-encapsulated PEI25k exhibi-ted a more significant reduction in cytotoxicity compared to PEI10k. Combined with the results of zeta potential experiments, it was shown that a significant reduction in the high surface positive charge of the PEI25k/DNA complex resulted in reduced cytotoxicity [43]. In the end, as observed in Fig. 3(b, d and f), the other polymers had the similar effect on cell survival in HEK-293T cells. In sum, after cell membrane encap-sulation, the cytotoxicity of PEI/DNA complex was significantly reduced, therefore providing the proper safety for this gene delivery vector.

3.10. In Vitro Cellular Uptake of RAWm-PDc and RBCm-PDc

As the ideal gene delivery vectors should have high cell uptake efficiency, the in vitro cellular uptake efficiency of RAWm-PDc and RBCm- PDc complexes in HEK-293T and HeLa cells was investigated via fluo-rescent microscopy and flow cytometry. As observed in Fig. 4 (c), the complete overlapping of red and green fluorescence indicated that FITC labeled PEI/DNA complex was fully encapsulated by Dil stained cell membrane, which further implied cell membrane encapsulated PEI complex was successfully prepared. In addition, FITC and Dil labeled RAWm-PDc or RBCm-PDc (Dil-FITC-RAWm-PDc/Dil-FITC-RBCm-PDc) complex was partially co-localized with DAPI stained nucleus, or distributed around cell nucleus, this result suggested the complexes with different mass ratios were efficiently absorbed into cells, and partially entered into nucleus. Also, the fluorescent intensity of RAWm-PDc and

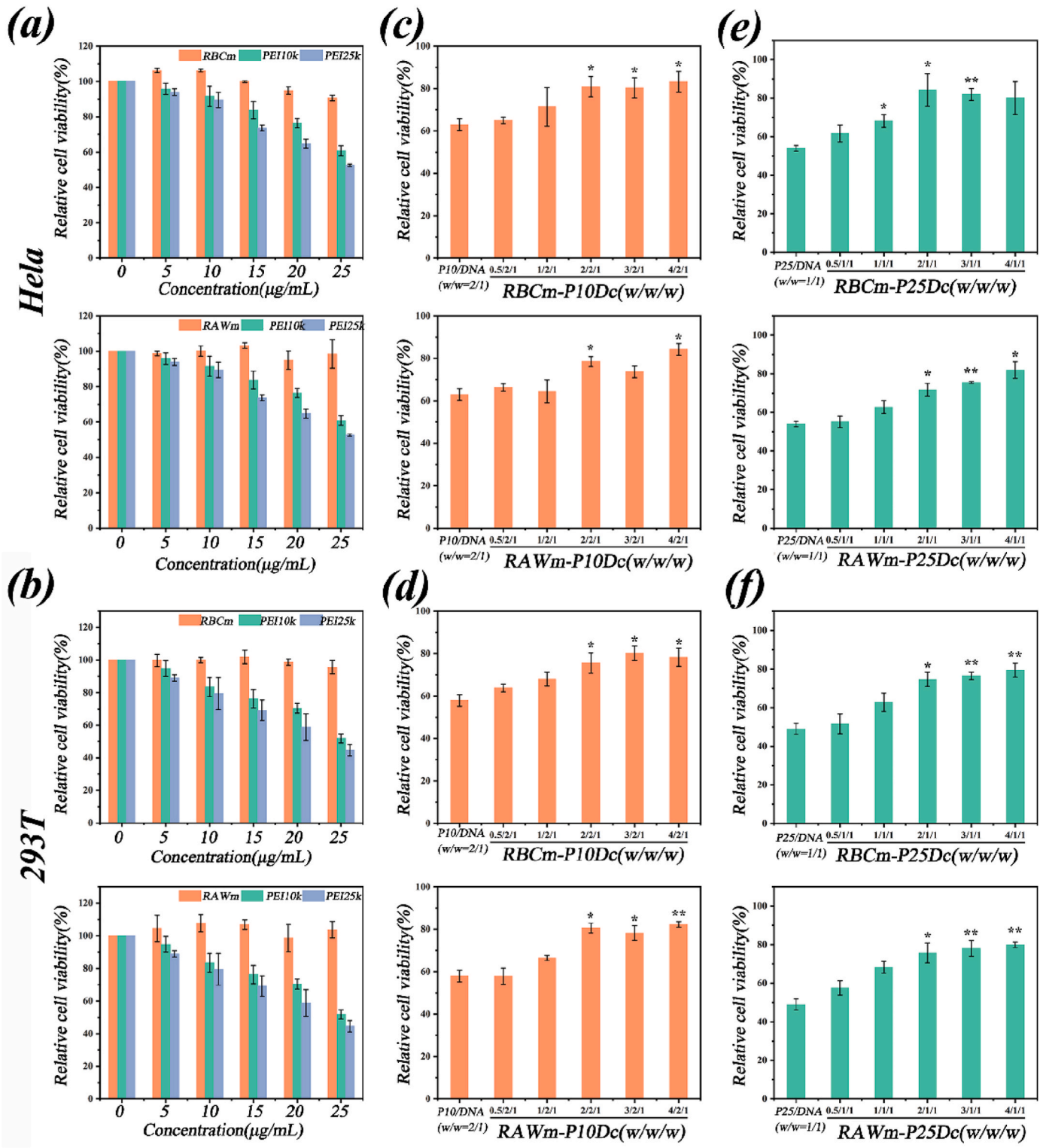

Fig. 3. MTT assay to measure cytotoxicity of complexes. (a) Relative cell viability of Hela cells that were treated with RBCm, RAWm, PEI10k and PEI25k under different concentrations. (b) Relative cell viability of HEK-293T cells that were treated with RBCm, RAWm, PEI10k and PEI25k under different concentrations. (c) Relative cell viability of Hela cells that were treated with RBCm-P10Dc and RAWm-P10Dc with different mass ratios. (d) Relative cell viability of HEK-293T cells that were treated with RBCm-P10Dc and RAWm-P10Dc with different mass ratios. (e) Relative cell viability of Hela cells that were treated with RBCm-P25Dc and RAWm-P25Dc with different mass ratios. (f) Relative cell viability of HEK-293T cells that were treated with RBCm-P25Dc and RAWm-P25Dc with different mass ratios. (Mean ± SD, n = 3; $^{*}P \leq 0.05$, $^{**}P \leq 0.01$).

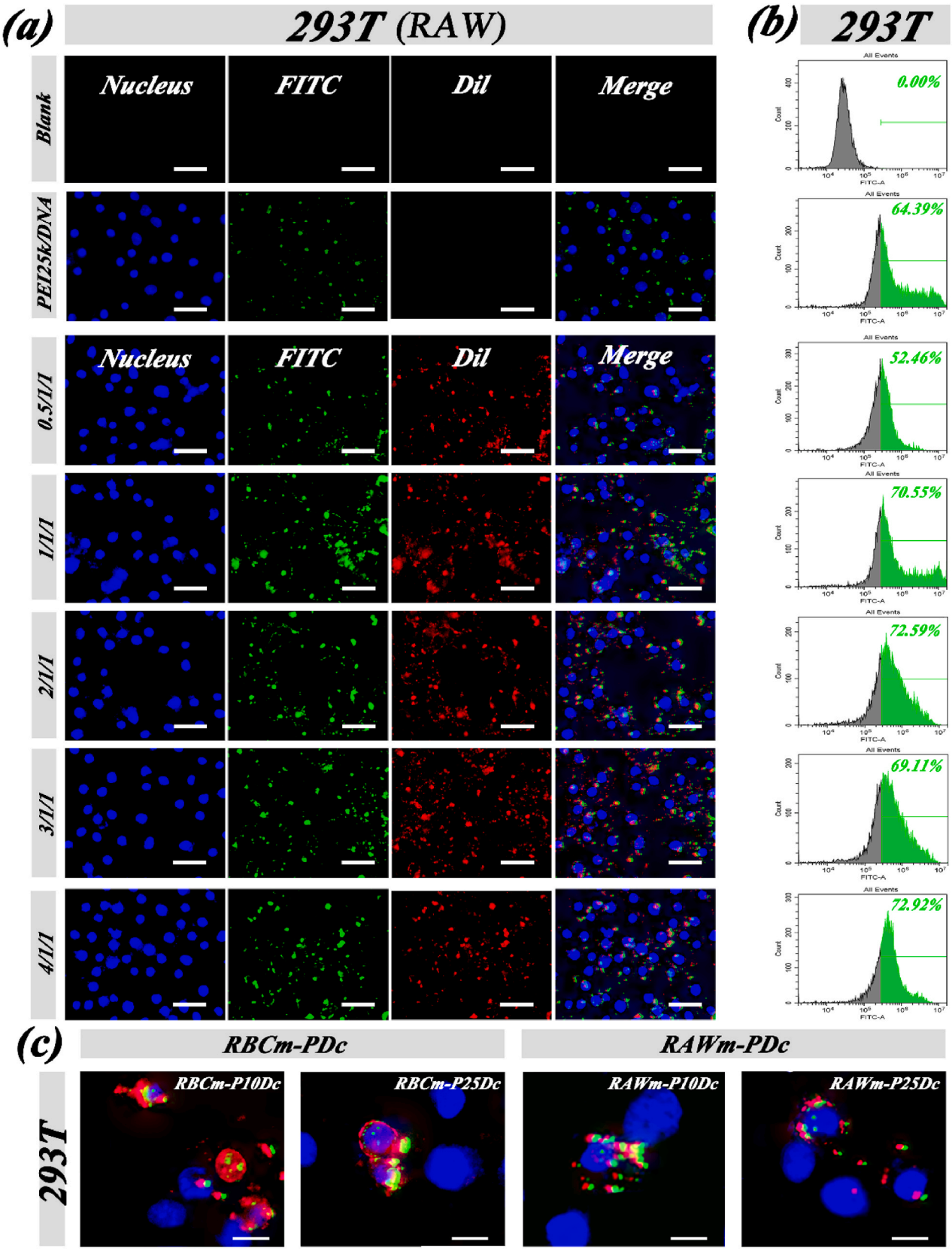

Fig. 4. In Vitro Cellular Uptake of RAWm-P25Dc in HEK-239T cells. (a) Fluorescence images (400 ×) of HEK-293T cells treated by Dil-FITC-RAWm-P25Dc complexes. (Scale bar = 50 μm). (b) FCM results of the uptake efficiency of Dil-FITC-RAWm-P25Dc complexes. (c) CLSM images (400 ×) of HEK-293T cells treated by Dil-FITC-RBCm-PDc and Dil-FITC-RAWm-PDc complexes. (Scale bar = 50 μm). Blue represents cell nucleus after DAPI staining, green represents FITC-labeled PEI, and red represents Dil-labeled RAW cell membranes/RBC cell membranes. (For interpretation of the references to color in this figure legend, the reader is referred to the Web version of this article.)

RBCm-PDc complex around the cell nucleus was elevated when the mass ratio increased, which indicating the increased mass ratio resulted in the more efficient cell membrane encapsulation and better cellular uptake. Meanwhile, In the same cell line and with same mass ratio, RAWm-P25Dc/DNA or RBCm-P25Dc/DNA complex exhibited higher fluorescent intensity, compared to RAWm-P10Dc/DNA or RBCm-P10Dc/DNA complex, which demonstrated the cellular uptake of RAWm-P25Dc/DNA and RBCm-P25Dc/DNA complex was more efficient.

Encouragingly, the obtained RBCm-PDc complexes exhibited excellent cellular uptake efficiencies.The maximum cellular uptake efficiencies of RBCm-P10Dc and RBCm-P25Dc in HEK-293T cells were 71.69 % (Fig. 5b) and 78.69 % (Fig. 6b), respectively, which were higher than those of the corresponding molecular weights of PEIs (57.14 % for PEI10k and 64.73 % for PEI25k).The RAWm-PDc complexes showed a similar profile in HEK-293T cells. The maximum cellular uptake efficiencies of 63.34 % (Fig. S4b) and 74.12 % (Fig. S5b) for RBCm-P10Dc

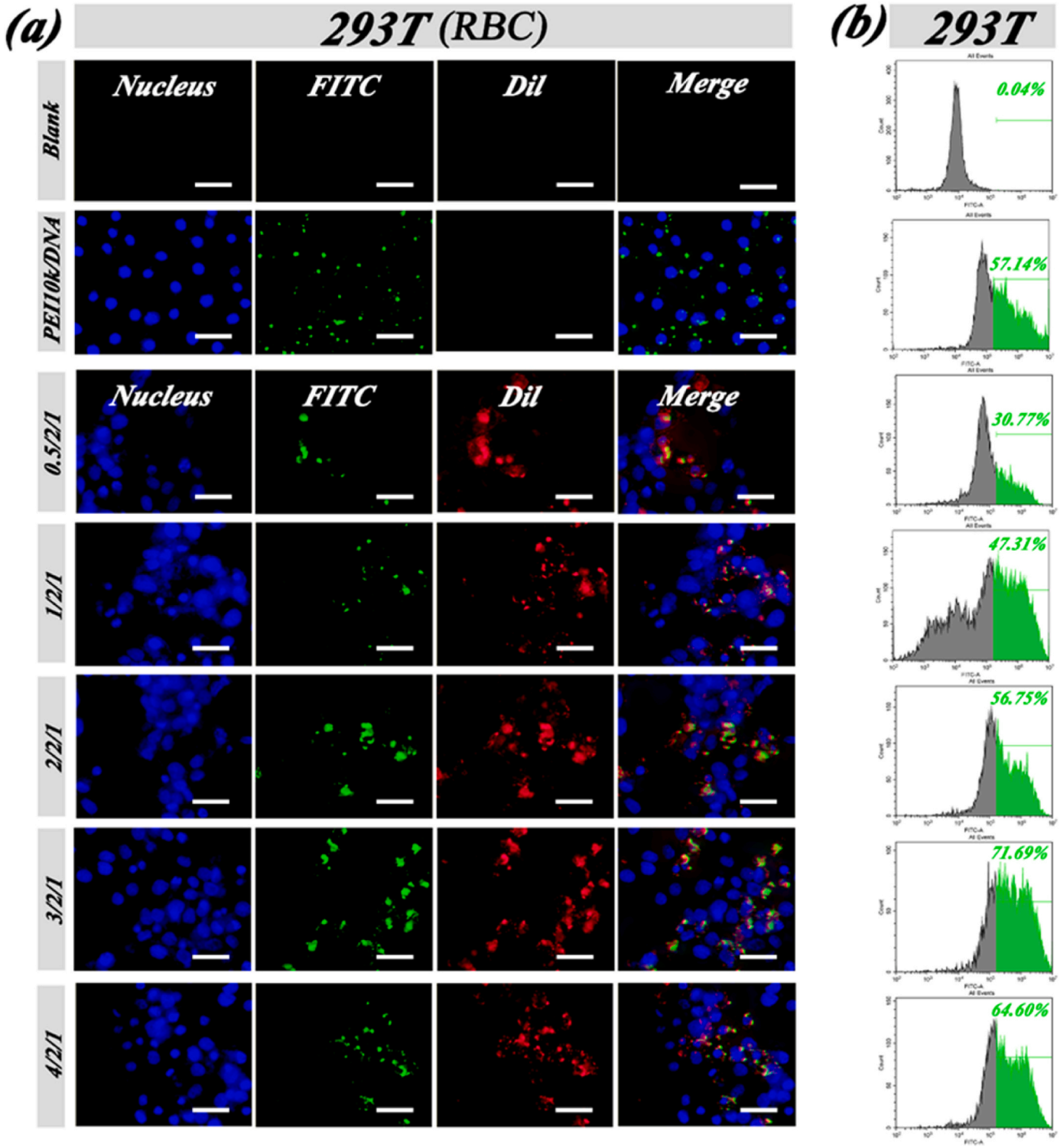

Fig. 5. Cell uptake results of RBCm-P10Dc complexes in HEK-239T cells. (a) Fluorescence images (400 ×) of HEK-293T cells treated by Dil-FITC-RBCm-P10Dc complexes. (Scale bar = 50 μm). (b) FCM results of the uptake efficiency of Dil-FITC-RBCm-P10Dc complexes.

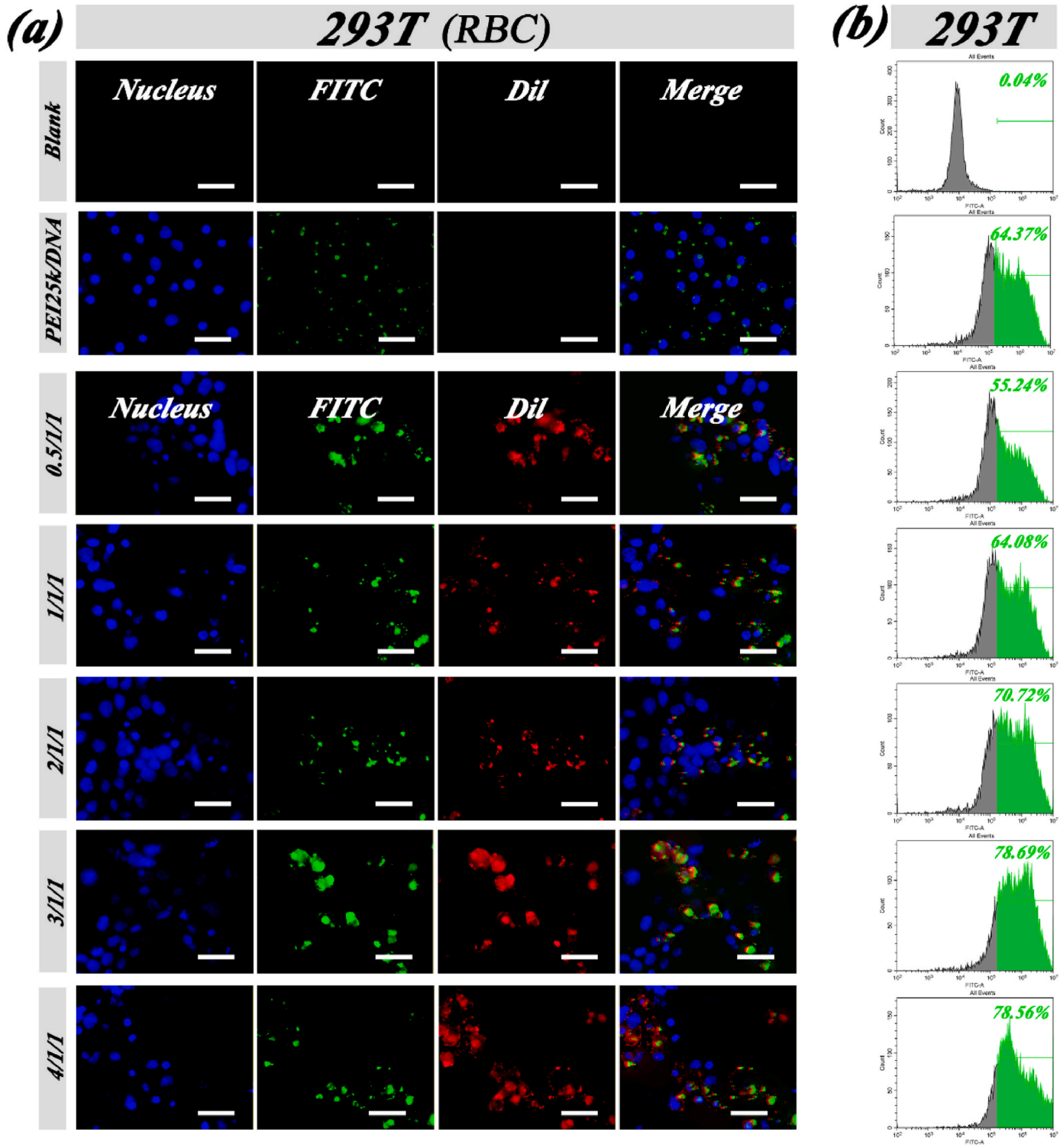

Fig. 6. Cell uptake results of RBCm-P25Dc complexes in HEK-239T cells. (a) Fluorescence images (400 ×) of HEK-293T cells treated by Dil-FITC-RBCm-P10Dc complexes. (Scale bar = 50 μm). (b) FCM results of the uptake efficiency of Dil-FITC-RBCm-P10Dc complexes.

and RBCm-P25Dc in Hela cells, respectively, were lower than those in HEK-293T cells. Comprehensive analysis of the results of cytotoxicity experiments showed that cell membrane encapsulation reduced the cytotoxicity of PEI/DNA complexes, which was more pronounced for the enhancement of the survival of HEK-293T cells. As a result, the complexes enhanced the cellular uptake efficiency in HEK-293T cells more significantly.

In conclusion, the cell membrane encapsulation strategy can effectively improve the cellular uptake efficiency, and the RBCm-PDc complex has a higher cellular uptake rate than the RAWm-PDc complex from an overall point of view, which makes the RBCm-PDc complex even more potential to be a safe and effective gene carrier.

3.11. In Vitor Gene Transfection of RAWm-PDc and RBCm-PDc

To address the transfection efficiency of RAWm-PDc and RBCm-PDc,

EGFP plasmid was used as the reporter gene, fluorescent microscopy and flow cytometry were exploited to measure the transfection efficiency in HEK-293T and Hela cells. As shown in Fig. 7–8 and Fig. S6-S7, the polymer/DNA complex was successfully entered into cells and GFP was intensively expressed. The transfection efficiency of the vector varied among the cell lines, with HEK-293T cells being more efficient compared to Hela cells, but both were less efficient than commercial reagents (Fig. 7c–S6c). In the same cell line and at same mass ratio, RAWm-P25Dc and RBCm-P25Dc had higher transfection efficiency than RAWm-P10Dc and RBCm-P10Dc. This is further corroborated by the mean fluorescence intensity trends of HEK-293T(Fig. 7d, e, 8d and 8e) and HeLa cells (Fig. S6d, S6e, S7d and S7e) transfected with the complex.

In the RAWm coated complexes, RAWm-P10Dc and RAWm-P25Dc achieved the highest efficiency of 43.47 % (Fig. 7a) and 62.81 % (Fig. 7b), respectively, which were higher than that of PEI10k/DNA and PEI25k/DNA. Furthermore, the transfection efficiency was elevated along with the increased mass ratio, and eventually decreased after reaching the maximal value. The similar result was observed in RBCm coated polymers, the maximal efficiency of RBCm-P10Dc and RBCm-P25Dc were 49.65 % (Fig. 8a) and 64.36 % (Fig. 8b) in HEK-293T cells, 8.96 % (Fig. S7a) and 15.91 % (Fig. S7b) in Hela cells, respectively. Compared to RAWm coating, RBCm coated polymers had higher efficiency both in HEK-293T and Hela cells. Importantly, the data obtained from fluorescent microscopy measurement was consistent with that from flow cytometry assay. All the data demonstrated cell membrane encapsulation can efficiently improve the transfection efficiency, and RBCm coating had better effect on transfection compared to RAWm coating.

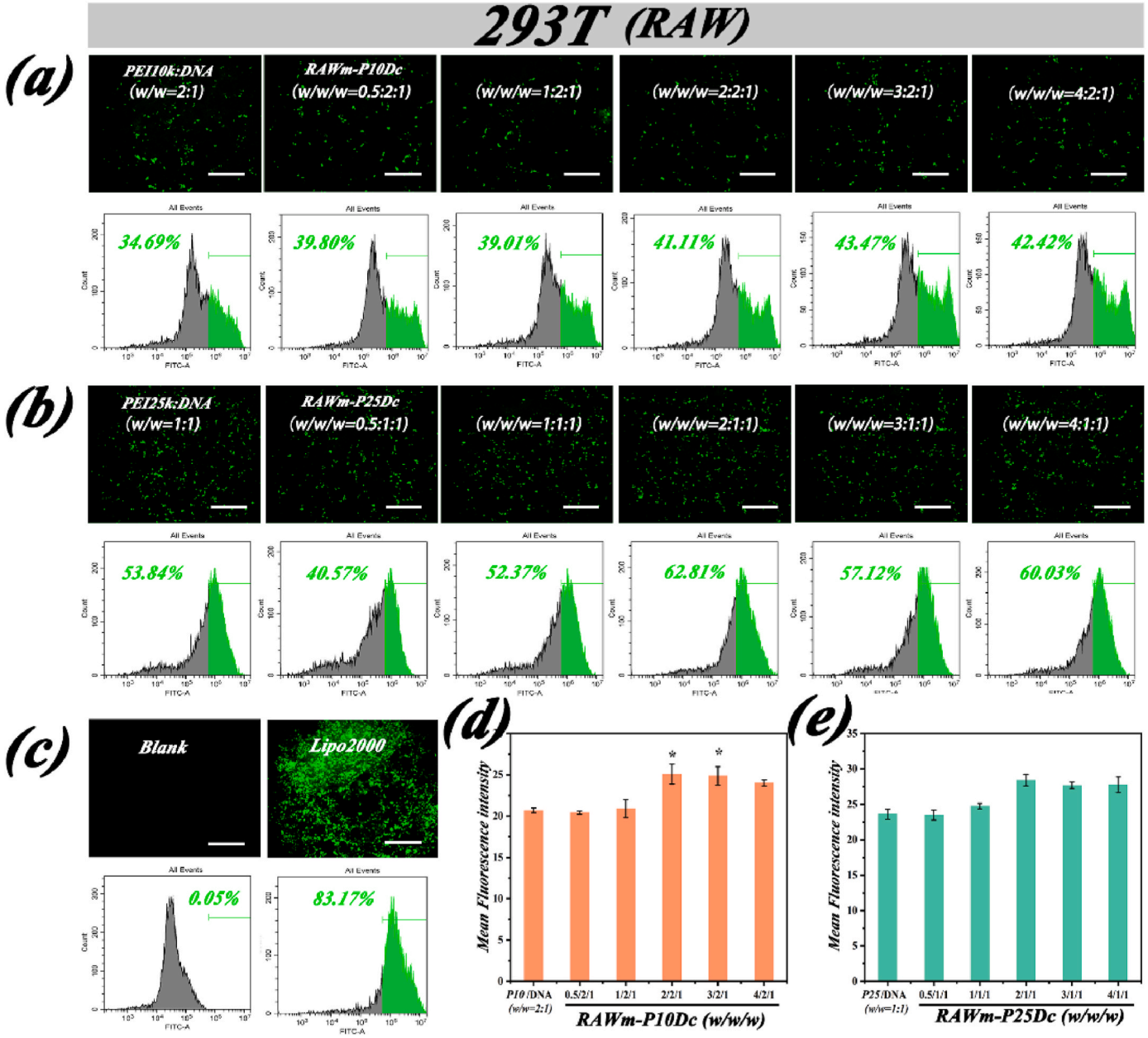

Fig. 7. Transfection results of RAWm-PDc complexes in HEK-293T cells. Transfection results of (a) RAWm-P10Dc, (b) RAWm-P25Dc with different mass ratios. (c) Transfection results of blank control and Lipo2000. Histogram analysis of transfection efficiency of RAWm-P10Dc (d) and RAWm-P25Dc (e) with different mass ratios. Scale bar = 1000 μm (mean ± SD, n = 3; *$P \leq 0.05$) .

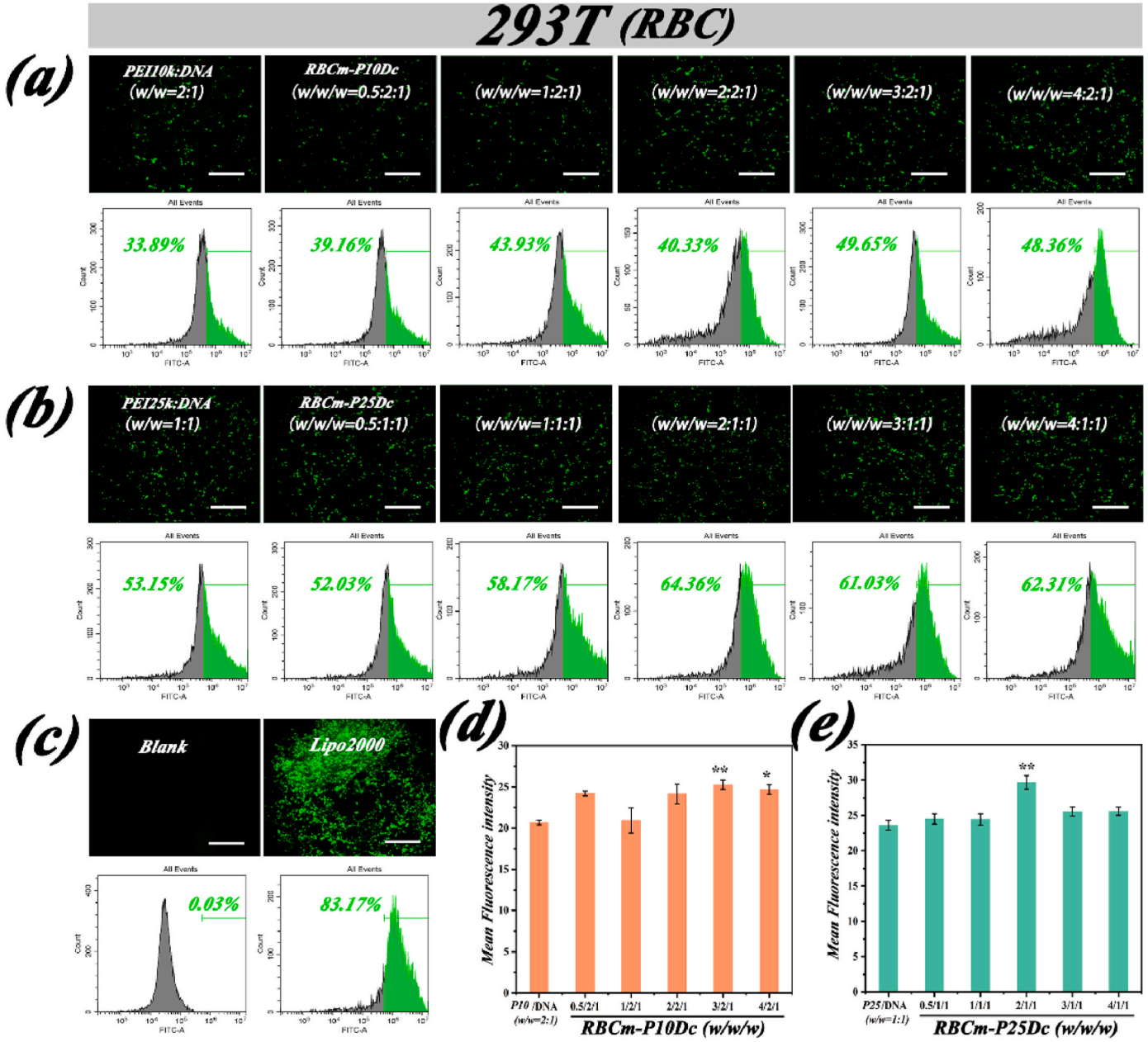

Fig. 8. Transfection results of RBCm-PDc complexes in HEK-293T cells. Transfection results of (a) RAWm-P10Dc, (b) RAWm-P25Dc with different mass ratios. (c) Transfection results of blank control and Lipo2000. Histogram analysis of transfection efficiency of RAWm-P10Dc (d) and RAWm-P25Dc (e) with different mass ratios. Scale bar = 1000 μm (mean ± SD n = 3;*$P \leq 0.05$, **$P \leq 0.01$) .

4. Conclusion

This work reports a straightforward and effective cell membrane coating modification strategy that could successfully reduce the cytotoxicity caused by the cationic charge density of PEI, as well as improve the cellular uptake efficiency of PEI/DNA complexes. SDS-PAGE and AFM measurements indicated that encapsulation of PEI/DNA complexes by RBCm/RAWm was successfully achieved. The non-specific protein adsorption behavior of the particles was investigated by using BSA protein as a model protein, which demonstrated that the cell membrane encapsulation strategy could effectively inhibit the non-specific protein adsorption of nanoparticles. Meanwhile, the RAWm-PDc/RBCm-PDc complex was able to demonstrate satisfactory stability over 7 days. The transfection assay using GFP as indicator has revealed that cell membrane coated PEI complex had significantly enhanced gene delivery efficiency. In sum, the RAWm-PDc/RBCm-PDc complex developed in this work can be regarded as a safe and effective gene delivery tool, further exploring the application of cell membranes as a safe material in gene delivery. In order to utilize the functions of different cells, multiple cell membrane-encapsulated NPs can also be used for targeted and synergistic therapies, potentially providing multiple functions and advantages for the treatment of various diseases. Although there are many challenges in transforming cell membrane-encapsulated nanoparticles into delivery vehicles for clinical applications, a wide range of applied research prospects and opportunities remain.

CRediT authorship contribution statement

Mengying Wang: Formal analysis, Investigation, Methodology, Validation, Writing – original draft. **Yanlin Sun:** Conceptualization, Methodology, Project administration, Resources, Supervision, Writing – review & editing. **Mingjie Wang:** Formal analysis, Methodology,

Validation. **Zhaojun Yang:** Investigation, Methodology. **Yong Shi:** Investigation, Methodology. **Dong Zeng:** Data curation, Supervision. **Liang Liu:** Funding acquisition, Resources, Supervision.

Declaration of competing interest

The authors declare that they have no known competing financial interests or personal relationships that could have appeared to influence the work reported in this paper.

Data availability

No data was used for the research described in the article.

Acknowledgments

This work was financially supported by the National Natural Science Foundation of China (21602166), Natural Science Foundation of Hubei Province (2020CFB760) and Research and Innovation Initiatives of WHPU (2021Y11).

Appendix A. Supplementary data

Supplementary data to this article can be found online at https://doi.org/10.1016/j.jddst.2024.105376.

References

[1] E.M. McErlean, C.M. McCrudden, H.O. McCarthy, Delivery of nucleic acids for cancer gene therapy: overcoming extra- and intra-cellular barriers, Ther. Deliv. 7 (2016) 619–637.
[2] F. Arabi, V. Mansouri, N. Ahmadbeigi, Gene therapy clinical trials, where do we go? An overview, Biomed. Pharmacother. 153 (2022).
[3] T. Wirth, S. Yla-Herttuala, Gene therapy used in cancer treatment, Biomedicines 2 (2014) 149–162.
[4] J. Chen, Q. Li, Y. Zhang, P. Yang, Y. Zong, S. Qu, Z. Liu, Oleic acid decreases the expression of a cholesterol transport-related protein (NPC1L1) by the induction of endoplasmic reticulum stress in CaCo-2 cells, J. Physiol. Biochem. 67 (2011) 153–163.
[5] M. Eisenstein, GENE EDITING to cut is to cure, Nature 557 (2018) S42–S43.
[6] H. Zu, D.C. Gao, Non-viral vectors in gene therapy: recent development, challenges, and prospects, AAPS J. 23 (2021).
[7] R.G. Sargent, S. Kim, D.C. Gruenert, Oligo/polynucleotide-based gene modification: strategies and therapeutic potential, Oligonucleotides 21 (2011) 55–75.
[8] S.-B. Yong, J.Y. Chung, Y. Song, Y.-H. Kim, Recent challenges and advances in genetically-engineered cell therapy, J. Pharm. Investigat. 48 (2018) 199–208.
[9] P. Seth, Vector-mediated cancer gene therapy - an overview, Cancer Biol. Ther. 4 (2005) 512–517.
[10] N.F. Sun, Z.A. Liu, W.B. Huang, A.L. Tian, S.Y. Hu, The research of nanoparticles as gene vector for tumor gene therapy, Crit. Rev. Oncol.-Hematol. 89 (2014) 352–357.
[11] U. Bezeljak, Cancer gene therapy goes viral: viral vector platforms come of age, Radiol. Oncol. 56 (2022) 1–13.
[12] B. Balakrishnan, E. David, Biopolymers augment viral vectors based gene delivery, J. Biosci. 44 (2019).
[13] B. Caffery, J.S. Lee, A.A. Alexander-Bryant, Vectors for glioblastoma gene therapy: viral & non-viral delivery strategies, Nanomaterials 9 (2019).
[14] Y. Kaneda, Y. Tabata, Non-viral vectors for cancer therapy, Cancer Sci. 97 (2006) 348–354.
[15] Q.Q. Zheng, D.Q. Lin, L. Lei, X.Y. Li, S. Shi, Engineered non-viral gene vectors for combination cancer therapy: a review, J. Biomed. Nanotechnol. 13 (2017) 1565–1580.
[16] S. Patil, Y.G. Gao, X. Lin, Y. Li, K. Dang, Y. Tian, W.J. Zhang, S.F. Jiang, A. Qadir, A.R. Qian, The development of functional non-viral vectors for gene delivery, Int. J. Mol. Sci. 20 (2019).
[17] C.C. Conwell, L. Huang, Recent advances in non-viral gene delivery, in: L. Huang, M.C. Hung, E. Wagner (Eds.), Non-Viral Vectors for Gene Therapy, second ed.: Part 12005, pp. 3-18..
[18] S. Taranejoo, J. Liu, P. Verma, K. Hourigan, A review of the developments of characteristics of PEI derivatives for gene delivery applications, J. Appl. Polym. Sci. 132 (2015).
[19] W.T. Godbey, K.K. Wu, A.G. Mikos, Poly(ethylenimine) and its role in gene delivery, J. Contr. Release : Off. J. Control. Release Soc. 60 (1999) 149–160.
[20] X. Wang, D.C. Niu, C. Hu, P. Li, Polyethyleneimine-based nanocarriers for gene delivery, Curr. Pharmaceut. Des. 21 (2015) 6140–6156.
[21] J.L. Merlin, A. N'Doye, T. Bouriez, G. Dolivet, Polyethylenimine derivatives as potent nonviral vectors for gene transfer, Drug News Perspect. 15 (2002) 445–451.
[22] K. Nam, S. Jung, J.P. Nam, S.W. Kim, Poly(ethylenimine) conjugated bioreducible dendrimer for efficient gene delivery, J. Contr. Release 220 (2015) 447–455.
[23] S.H. Wu, D.N. Ni, Y.J. Yan, X.H. Pan, X. Chen, J.T. Guan, X.M. Xiong, L. Liu, Safe and efficient gene delivery based on rice bran polysaccharide, Int. J. Biol. Macromol. 137 (2019) 1041–1049.
[24] Y.R. Chen, C.B. Liu, Z.J. Yang, Y.L. Sun, X. Chen, L. Liu, Fabrication of zein-based hydrophilic nanoparticles for efficient gene delivery by layer-by-layer assembly, Int. J. Biol. Macromol. 217 (2022) 381–397.
[25] S.H. Wen, F.Y. Zheng, M.W. Shen, X.Y. Shi, Surface modification and PEGylation of branched polyethyleneimine for improved biocompatibility, J. Appl. Polym. Sci. 128 (2013) 3807–3813.
[26] L. Liu, Z.J. Yang, C.B. Liu, M.Y. Wang, X. Chen, Preparation of PEI-modified nanoparticles by Active Ingredient self-polymerization for efficient DNA delivery, Biotechnol. Appl. Biochem. 70 (2023) 824–834.
[27] Z.H. Guo, Y.J. Li, Y.G. Fu, T.Q. Guo, X. Li, S. Yang, J. Xie, Enhanced antisense oligonucleotide delivery using cationic liposomes incorporating fatty acid-modified polyethylenimine, Curr. Pharmaceut. Biotechnol. 15 (2014) 800–805.
[28] L. Liang, Y. Yujian, N. Danni, W. Shuheng, C. Yiran, C. Xin, X. Xuemin, L. Gang, TAT-functionalized PEI-grafting rice bran polysaccharides for safe and efficient gene delivery, Int. J. Biol. Macromol. 146 (2020) 1076–1086.
[29] X.F. Hao, Q. Li, H.N. Wang, K. Muhammad, J.T. Guo, X.K. Ren, C.C. Shi, S.H. Xia, W.C. Zhang, Y.K. Feng, Red-blood-cell-mimetic gene delivery systems for long circulation and high transfection efficiency in ECs, J. Mater. Chem. B 6 (2018) 5975–5985.
[30] S. Han, Y. Lee, M. Lee, Biomimetic cell membrane-coated DNA nanoparticles for gene delivery to glioblastoma, J. Contr. Release 338 (2021) 22–32.
[31] Z.Q. Zhang, D. Li, X.H. Li, Z.H. Guo, Y.L. Liu, X. Ma, S.Z. Zheng, PEI-modified macrophage cell membrane-coated PLGA nanoparticles encapsulating Dendrobium polysaccharides as a vaccine delivery system for ovalbumin to improve immune responses, Int. J. Biol. Macromol. 165 (2020) 239–248.
[32] C. Sabu, C. Rejo, S. Kotta, K. Pramod, Bioinspired and biomimetic systems for advanced drug and gene delivery, J. Contr. Release 287 (2018) 142–155.
[33] W.Y. Zhang, M. Zhao, Y.L. Gao, X. Cheng, X.Y. Liu, S.K. Tang, Y.B. Peng, N. Wang, D.D. Hu, H.S. Peng, J.Q. Zhang, Q. Wang, Biomimetic erythrocytes engineered drug delivery for cancer therapy, Chem. Eng. J. 433 (2022).
[34] Z. Fang, M. Zhang, R. Kang, M.X. Cui, M.D. Song, K.H. Liu, A cancer cell membrane coated nanoparticles-based gene delivery system for enhancing cancer therapy, Int. J. Pharm. 629 (2022).
[35] L. Liu, Y.R. Chen, C.B. Liu, Y.J. Yan, Z.J. Yang, X. Chen, G. Liu, Effect of extracellular matrix coating on cancer cell membrane-encapsulated polyethyleneimine/DNA complexes for efficient and targeted DNA delivery in vitro, Mol. Pharm. 18 (2021) 2803–2822.
[36] M. Pereira-Silva, A.C. Santos, J. Conde, C. Hoskins, A. Concheiro, C. Alvarez-Lorenzo, F. Veiga, Biomimetic cancer cell membrane-coated nanosystems as next-generation cancer therapies, Expet Opin. Drug Deliv. 17 (2020) 1515–1518.
[37] W.L. Song, P.F. Jia, T. Zhang, K.K. Dou, L.B. Liu, Y.P. Ren, F.J. Liu, J.M. Xue, M. S. Hasanin, H.Z. Qi, Q.H. Zhou, Cell membrane-camouflaged inorganic nanoparticles for cancer therapy, J. Nanobiotechnol. 20 (2022).
[38] C.M.J. Hu, L. Zhang, S. Aryal, C. Cheung, R.H. Fang, L.F. Zhang, Erythrocyte membrane-camouflaged polymeric nanoparticles as a biomimetic delivery platform, Proc. Natl. Acad. Sci. U.S.A. 108 (2011) 10980–10985.
[39] C. Gao, Q.X. Huang, C.H. Liu, C.H.T. Kwong, L.D. Yue, J.B. Wan, S.M.Y. Lee, R. B. Wang, Treatment of atherosclerosis by macrophage-biomimetic nanoparticles via targeted pharmacotherapy and sequestration of proinflammatory cytokines, Nat. Commun. 11 (2020).
[40] F.F. Liu, Z.L. Dong, M.R. Li, J.H. Sun, Z.Y. Hou, A. Younas, X.L. Wan, H.T. Shang, N. Zhang, A macrophage plasma membrane-coated and DNA structured nanomedicine targets to alleviate rheumatoid arthritis via dual inhibition to TNF-α and NF-κB, Int. J. Pharm. 642 (2023).
[41] K.K. Ying, Y.F. Zhu, J.Q. Wan, C.Y. Zhan, Y.C. Wang, B.B. Xie, P.R. Xu, H.M. Pan, H.X. Wang, Macrophage membrane-biomimetic adhesive polycaprolactone nanocamptothecin for improving cancer-targeting efficiency and impairing metastasis, Bioact. Mater. 20 (2023) 449–462.
[42] Y. Zhang, K.M. Gai, C. Li, Q. Guo, Q.J. Chen, X. He, L.S. Liu, Y.J. Zhang, Y.F. Lu, X. L. Chen, T. Sun, Y.Z. Huang, J.J. Cheng, C. Jiang, Macrophage-membrane-coated nanoparticles for tumor-targeted chemotherapy, Nano Lett. 18 (2018) 1908–1915.
[43] X.R. Shao, X.Q. Wei, X. Song, L.Y. Hao, X.X. Cai, Z.R. Zhang, Q. Peng, Y.F. Lin, Independent effect of polymeric nanoparticle zeta potential/surface charge, ontheir cytotoxicity and affinity to cells, Cell Prolif. 48 (2015) 465–474.